Enhancement of field generation via maximal atomic coherence prepared by fast adiabatic passage in Rb vapor

V. A. Sautenkov,[1,3] C. Y. Ye,[1] Y. V. Rostovtsev,[1] G. R. Welch,[1] and M. O. Scully[1,2]

[1]*Institute for Quantum Studies and Department of Physics, Texas A&M University, College Station, Texas 77843, USA*
[2]*Department of Chemistry, Princeton University, Princeton, New Jersey 08544, USA*
[3]*Lebedev Institute of Physics, Moscow 117924, Russia*

We have experimentally demonstrated the enhancement of coherent Raman scattering in Rb atomic vapor by exciting maximal atomic coherence with fractional stimulated Raman adiabatic passage. Experimental results are in good agreement with numerical simulations. The results support the possibility of increasing the sensitivity of coherent anti-Stokes Raman spectroscopy by preparing maximal atomic or molecular coherence using short pulses.

I. INTRODUCTION

Although four-wave mixing processes have been studied for at least 25 years [1,2], it has only recently been shown that quantum coherence can dramatically increase the nonlinear response in atomic, molecular, or solid-state media without overwhelming absorption [3–7]. Currently the subject of quantum coherence is the focus of broad research, including quantum computing and quantum state storage [8–10], manipulation of single quanta [11–13]; in a coherently prepared medium with maximal coherence there occur effective frequency conversion [14,15], subfemtosecond pulse generation [16], and enhanced coherent anti-Stokes spectroscopy (CARS) [17].

Maximal coherence in atoms and molecules can be created with a pair of short coupling pulses which adiabatically interact with an atomic or molecular system as depicted in Fig. 1. By choosing the proper time dependence of the pulses shown in Fig. 1(a), a 100% population transfer between lower levels can be achieved. This is referred to as stimulated Raman adiabatic passage, or STIRAP [18–21]. However, using the time dependence shown in Fig. 1(b), referred to as fractional STIRAP (to distinguish the technique from STIRAP) we can create maximal coherence between the lower levels.

In this paper, we report an experimental implementation of fractional STIRAP in a Rb vapor cell slightly above room temperature where lower level coherence is created between Zeeman sublevels. We demonstrate coherent Raman scattering in the Rb vapor using short laser pulses (shorter than the lifetime of the excited state.) We observe the enhancement of the coherent Raman scattering under the condition of maximal coherence between Zeeman sublevels prepared by fractional STIRAP. The observed intensity of the signal pulse depends quadratically on the density of Rb atoms. We theoretically predict this behavior, and show that the experiments are in agreement with numerical simulations.

The essence of the technique is the following. Two coupling pulses (with duration less than the lifetime of the excited state), with Rabi frequencies Ω_1 and Ω_2 resonant with transitions a-c and a-b (see Fig. 1), create coherence between levels b and c. After some time, (less than the lifetime of the lower level coherence) the probe pulse Ω_3 arrives and scatters from the atomic coherence ρ_{bc} leading to efficient generation of a signal field Ω_4. The important points are that the frequency of the signal field is shifted exactly to the transition frequency between levels b and c, and the intensity of the signal field depends on the magnitude of the atomic coherence ρ_{bc}.
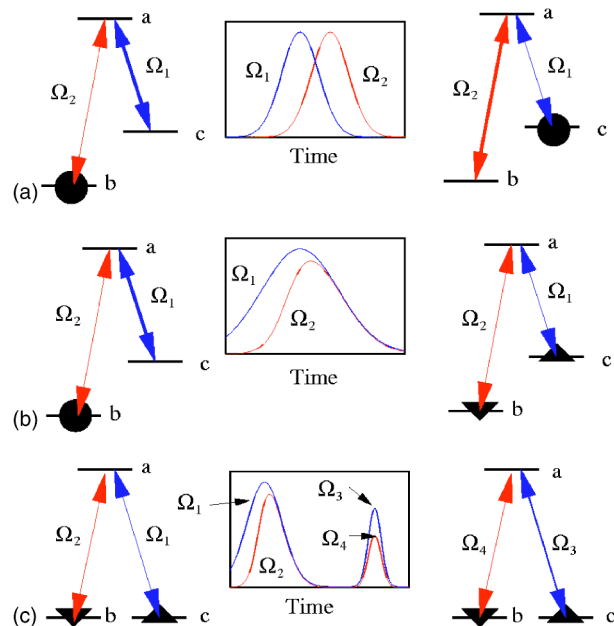

FIG. 1. (a) STIRAP. "Counterintuitive" pulse sequence transfers population from level b to c with 100% efficiency. (b) Fractional STIRAP. A pair of pulses with the same back edge distributes populations equally and excites maximal coherence between levels b and c. The coherence between levels is depicted by triangles. (c) Applying Ω_1 and Ω_2 to a three-level atom, one can excite maximal Zeeman coherence via fractional STIRAP. Field Ω_4 is generated via coherent scattering of probe field Ω_3.
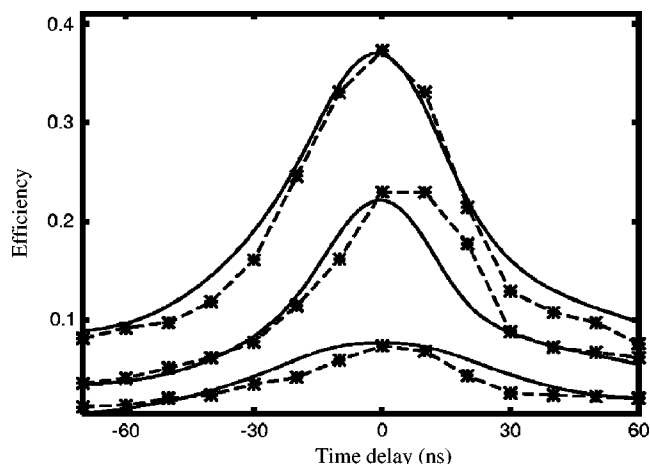
FIG. 2. Efficiency of generation of field Ω_4 mutual delay between coupling pulses for three different atomic densities. Zero delay was selected for the condition where the tails of the pulses coincide. Experimental results (dotted curve). Results of numerical simulations (solid curve).

FIG. 3. Experimental setup.

The main result of this paper is shown in Fig. 2. By changing the time delay, one can see that there is a maximum of the efficiency of generation of the signal field corresponding to the configuration of the coupling pulses that creates maximum coherence. It is this coherence that distinguishes the present technique from ordinary CARS where the coherence level is low.

An important feature of our experiments that distinguishes them from prior experiments, such as those on photon storage [8–10], is that the duration of the pulses are short in comparison with the relaxation rates of the associated optical transitions. Furthermore, in those experiments the magnitude of ρ_{bc} coherence was relatively low, and the duration of the pulses was long compared to the optical lifetime and comparable to the spin coherence lifetime. Note also that, because there is no inhomogeneous broadening of spin transition, our approach is different from the echo technique where the additional π pulses to control spin coherence are applied [22].

Also our work is different from the work done by the Harris group at Stanford where a very efficient technique employing maximal atomic coherence was developed. Their duration of pulse is longer than the optical relaxation time (duration of the laser pulses is 15 ns, while $T_1=5.2$ ns for level $6p7s\,^3P_1$ of ^{208}Pb). Thus, the laser field is practically quasi-stationary, and population of the dark state occurs via optical pumping rather than via rapid adiabatic passage. While in our experiments, we use a fractional STIRAP to create coherence between hyperfine levels, also the duration of pulses is shorter than the population relaxation of the excited state. Using the strong saturation regime gives one a very robust effect of coherence excitation between atomic levels.
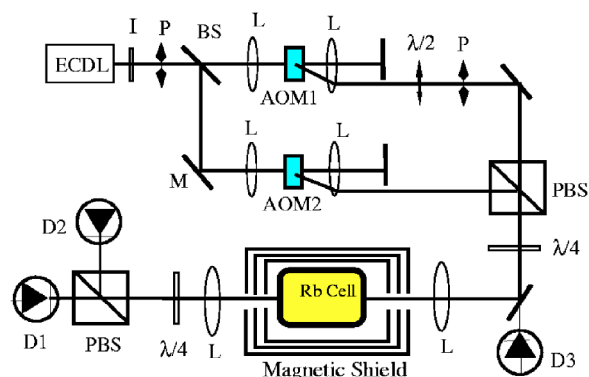
II. EXPERIMENT

A schematic diagram of the experimental setup is shown in Fig. 3. Radiation from an external-cavity diode laser is tuned to the D_1 transition of ^{87}Rb $5S_{1/2}$ ($F=2$) to $5P_{1/2}$ ($F'=1$). The beam is split by a beamsplitter and passes through acousto-optic modulators (AOM) driven by pulses with adjustable duration and delay (the rise time of the AOM is near 9 ns), and the same frequency shift (200 MHz). The optical path lengths for both beams are the same. The temporal behavior of the pulses is detected by fast photodiode D_3.

One beam serves as the first coupling pulse and the probe pulse. The time duration of the first coupling pulse is 150 ns, and that of the second pulse is 20 ns. The other beam, also of 20 ns duration, is used as the second coupling pulse. The front and tail slopes of the pulses are limited by the AOMs and are synchronized electronically. The polarization of the first beam (which includes the first coupling pulse and the probe pulse) is rotated by 90° relative to the polarization of the other pulse. These orthogonally polarized laser beams are combined by a polarizing beamsplitter.

The polarization of the pulses is modified by a $\lambda/4$ wave plate, which results in opposite circular polarization of the two pulses. The combined laser beams are focused by a lens (focus length 30 cm) into a cell of length 2.5 cm containing saturated Rb vapor with atomic density $N=1\times10^{11}$ cm^{-3}. The cell is installed in a three-layer magnetic shield. The atomic density is estimated from the temperature of the cell and corrected by absorption measurements [23]. After the cell, the transmitted laser beams with opposite circular polarizations are separated by a second $\lambda/4$ wave plate and another polarizing beamsplitter. The transmitted first coupling pulse and probe pulse are detected by fast photodiode D_1. The second coupling pulse and the generated signal pulse are detected by fast photodiode D_2. All fast photodiodes have identical characteristics with 1 ns resolution.

The coupling pulses create ground-state coherence in the atomic vapor. Then after some time delay, the pulse of probe field scatters on the atomic coherence to generate a new field (signal). Three different temporal combinations of the coupling pulses and the probe pulse are shown in Fig. 4.

The energy of the first coupling pulse is 375 pJ, and its duration is 150 ns, which was selected so that several optical
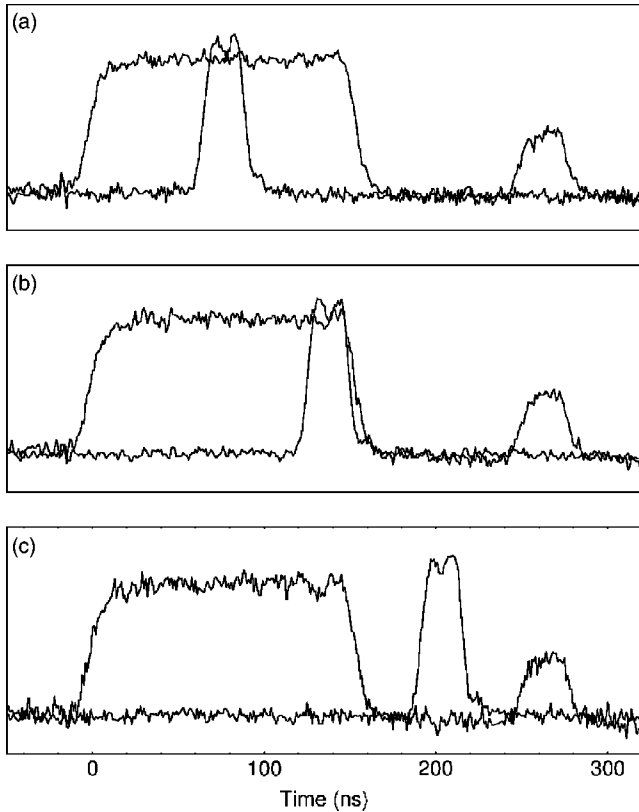
FIG. 4. Experimental pulse shapes recorded before propagation of the optical fields through the Rb cell. The noise level in these data is due to the electronics.
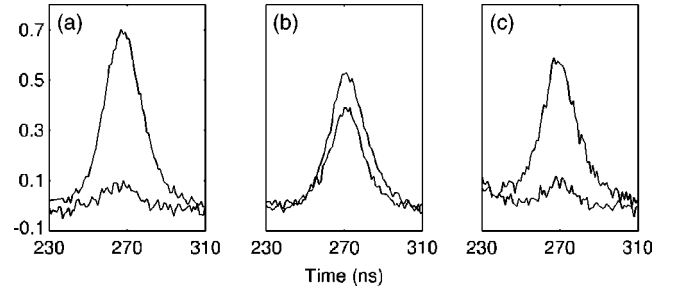

FIG. 5. Probe and generated signal fields after propagation through atomic vapor. In all figures, the probe field is stronger than the signal field. Amplitudes are normalized to the amplitude of the probe pulse before entering the cell. (b) demonstrates the maximal amplitude of the generated signal field obtained by the combination of preparation pulses shown in Fig. 4(b).

close to the maximal coherence. The intensity of the generated field is 0.37 of the intensity of the initial probe pulse.

Figure 2 shows the normalized intensity of the generated new field (signal) as a function of delay time between coupling pulses for three different densities $N=(1, 0.8, 0.4) \times 10^{11}$ cm^{-3}. Zero time delay corresponds the situation where the tails of the first and second coupling fields switched off simultaneously. This is the condition for obtaining effective fractional STIRAP and maximal coherence. One can see that the efficiency (the ratio of the signal intensity at the output of the cell to the intensity of probe field at the entrance of the cell) is proportional to the square of the atomic density.

pumping cycles can occur before the second coupling pulse is applied. The time delay between the end of the first coupling pulse and the probe pulse is 100 ns, which is considerably less than the ground-state coherence decay time of about 10^3 ns, and more than three times longer than the excited-state lifetime. The energy of the second coupling pulse is 50 pJ, and its duration of 20 ns is short enough to perform STIRAP for the time period less than the lifetime of the excited state (27 ns). The effective area of the laser beams is about 2×10^{-3} cm^2; the corresponding Rabi frequency for every beam is $\Omega = 10\gamma$ (where $\gamma = 1/\tau$ and $\tau = 27$ ns), so we fulfilled the condition

$$\tau\sqrt{\Omega_1^2 + \Omega_2^2} \geqslant 10 \tag{1}$$

(see in Ref. [18] for details).

Figure 5 shows the probe and signal fields after their propagation through the cell. The combination of coupling pulses shown in Figs. 4(a) and 4(c) is not optimal for a large ground-state coherence to remain after the pulses are gone. As a result, the corresponding signal fields in Figs. 5(a) and 5(c) have small amplitudes. The optimal signal (with maximum amplitude) shown in Fig. 5(b) is obtained by adjusting the time delay of the second coupling pulse relative to the first coupling pulse in such a way that the condition for fractional STIRAP is fulfilled. In this case, fractional STIRAP induces ground-state coherence, which is expected to be

III. THEORY

To gain physical insight into this process, we have performed numerical simulations for the propagation of the laser pulses in the medium. Using a circular polarized driving field, we optically pump the population in states $|F=2, M=+1\rangle$ and $|F=2, M=+2\rangle$, and then we apply short pulses to perform fractional STIRAP. Because the pulse duration is shorter than the natural decay time, and the Rabi frequencies are large enough [see Eq. (1)], the population is transfered by rather stimulated processes than by spontaneous transitions, and a three-level model is expected to provide a good description of the atomic configuration under consideration. Thus instead of the real physical energy level manifolds $[5S_{1/2}(F=2) \leftrightarrow 5P_{1/2}(F'=1)$ transition] we base our calculations on an idealized three-level system as depicted in Fig. 1(a). This three-level system provides us a simplification of the actual system justified by the agreement between simulations and experiment. The experiments are done near room temperature, so we assume that the ground states are equally populated before the coupling pulses are applied.

Consider a three-level system selectively coupled by three laser pulses. The first two are coupling pulses, and the third is a probe pulse. The two coupling fields, ε_1 and ε_2, with Rabi frequency Ω_1 and Ω_2, respectively, excite transitions $a \rightarrow c$ and $a \rightarrow b$. This generates coherence between levels b

and c. Somewhat later, the probe pulse ε_3, with Rabi frequency Ω_3, interacts with the medium. Because the medium already has coherence ρ_{bc}, coherent Raman scattering of the probe pulse leads to the generation of a signal pulse ε_4 with Rabi frequency Ω_4.

The interaction Hamiltonian in the rotating wave approximation for this system is

$$\hat{H} = \hbar\Delta_b|b\rangle\langle b| + \hbar\Delta_c|c\rangle\langle c| + \hat{V}_I, \qquad (2)$$

where

$$V_I = -\hbar[(\Omega_1 + \Omega_3)|a\rangle\langle c| + (\Omega_2 + \Omega_4)|a\rangle\langle b| + \text{H.c.}]. \quad (3)$$

$\Omega_i = \wp_i\varepsilon_i/\hbar$ is the Rabi frequency of the respective fields; $\wp_1$ is the electrical dipole matrix element between states a and b, $\wp_2$ – between states a and c; $\Delta_b = \omega_{ab} - \nu_1$ and $\Delta_c = \omega_{ac} - \nu_2$ are the laser detuning from the atomic resonances; ε_i is the amplitude of the respective laser field, and Δ_j is the laser detuning from the atomic resonance. The time-dependent density matrix equations of motion are

$$\dot{\rho}_{ab} = -\Gamma_{ab}\rho_{ab} + in_{ab}(\Omega_1 + \Omega_3) - i\rho_{cb}(\Omega_2^* + \Omega_4^*), \qquad (4)$$

$$\dot{\rho}_{ca} = -\Gamma_{ca}\rho_{ca} + in_{ca}(\Omega_2 + \Omega_4) + i\rho_{cb}(\Omega_1^* + \Omega_3^*), \qquad (5)$$

$$\dot{\rho}_{cb} = -\Gamma_{cb}\rho_{ab} + i\rho_{ca}(\Omega_1 + \Omega_3) - i\rho_{ab}(\Omega_2 + \Omega_4), \qquad (6)$$

$$\dot{n}_b = \gamma_b n_a + i\rho_{ba}(\Omega_1 + \Omega_3) - i\rho_{ab}(\Omega_1^* + \Omega_3^*), \qquad (7)$$

$$\dot{n}_c = \gamma_c n_a + i\rho_{ca}(\Omega_2^* + \Omega_4^*) - i\rho_{ac}(\Omega_2 + \Omega_4), \qquad (8)$$

where $\Gamma_{ab} = \gamma_{ab} + i\Delta_b$, $\Gamma_{ca} = \gamma_{ph} - i\Delta_c$, $\Gamma_{cb} = \gamma_{cb}$; and $n_\alpha = \rho_{\alpha\alpha}$ is the diagonal elements of density matrix; $n_{\alpha\beta} = n_\alpha - n_\beta$ is the population inversion between levels α and β. Solving these equations gives the time evolution of the density matrix. To form a self-consistent system of equations, one should add equations for field propagation, which are given by

$$\frac{\partial(\Omega_2 + \Omega_4)}{\partial\xi} = -i\eta_b\rho_{ab}, \qquad \frac{\partial(\Omega_1 + \Omega_3)}{\partial\xi} = -i\eta_c\rho_{ac}, \quad (9)$$

where $\eta_b = \nu_1 N\wp_b/(2\epsilon_0 c)$, $\eta_c = \nu_2 N\wp_c/(2\epsilon_0 c)$ are the coupling constants, $\nu_{1,2}$ are the frequencies of the fields, N is the density of medium, ϵ_0 is the permitivity of the vacuum, and c is the speed of light in vacuum. We use coordinates ξ and τ, which are related to the laboratory coordinates by $\xi = z$ and $\tau = t - z/c$.

IV. DISCUSSION

We performed numerical simulations of the above theory using the same values of the parameters as in the experiments. The results of these simulations are shown in Fig. 2 (solid curve). Experimental and theoretical curves show similar behavior except in the wings, and small differences are seen in the maxima. A residual signal at large delay time can be associated with the long tails of pulses and residual cw background of the optical fields.

We have also studied the power dependence of the generation of the signal field. The total power of the pulses was reduced by variable attenuator installed before the first beamsplitter. The conversion efficiency varies only slightly for large changes in power (from our maximum level to half) and then decreases very rapidly as power is further reduced. These measurements confirm that we have enough power for STIRAP. The good agreement between our experimental and theoretical results confirms that we have indeed obtained maximal coherence via fractional STIRAP and observed enhanced time-delayed stimulated Raman scattering with high efficiency. Fractional STIRAP is a robust technique to obtain maximum Raman scattering. We would like to note that we have also studied delayed Raman scattering at higher Rb densities, but we cannot obtain efficiency more than 0.4 due to the strong absorption and optical pumping to the other hyperfine level ($F = 1$) which is closed to the theoretical limit of 50% under our conditions (see [26]).

The developed technique takes advantage of the maximum coherence induced between lower atomic or molecular vibrational levels. Several methods can be used for the effective preparation of atomic coherence [17], such as coherent population trapping [24], chirped pulses, and the fractional STIRAP [25], which we use in this experiment.

Note that the delayed CARS is a universal technique that can be applied to either atoms or molecules in various environments (gas, liquid, and solids) and can be used in a practical time scale. Its important feature is the capability of determining vibrational frequencies in one laser pulse, assuming that the vibrational frequency is within the two-photon linewidth of the beat note of the applied fields (which can be larger than the natural linewidth of the optical transitions and the laser linewidth because of power broadening). That is significantly different from ordinary CARS where the frequency of signal field is determined by the four-photon resonance, and tuning the coupling frequency is essential to determine the splitting of the levels. In the developed technique, the atomic coherence created by the first pair of pulses is oscillating at the frequency difference of the lower levels, and, after some time delay, an anti-Stokes signal appears as scattering from the probe pulse. Thus, the frequency shift between the probe and signal fields is exactly the splitting between the b and c levels.

V. CONCLUSION

We have implemented fractional STIRAP in a Rb vapor cell to generate maximum coherence between Zeeman sublevels. We have theoretically predicted and experimentally demonstrated coherent Raman scattering using short laser pulses (shorter than the relaxation of lifetime of excited state). We observe an enhancement of coherent Raman scattering under the condition of maximal coherence prepared by fractional STIRAP in agreement with the numerical simulations. The observed intensity of the signal pulse depends quadratically on the density of Rb atoms. These results support the idea of a femtosecond adaptive spectroscopic technique using CARS [17], utilized in a femtosecond time scale in order to improve sensitivity of CARS measurements [27–29], which can be applied to various atomic, molecular, and biological systems.

ACKNOWLEDGMENTS

[1] R. W. Boyd, *Nonlinear Optics* (Academic, Boston, 1992).

[2] Y. R. Shen, *The Principles of Nonlinear Optics* (Wiley, New York, 1984).

[3] S. E. Harris, G. Y. Yin, M. Jain, and A. J. Merriam, Philos. Trans. R. Soc. London, Ser. A **355** (1733), 2291 (1997).

[4] A. J. Merriam, S. J. Sharpe, M. Shverdin, D. Manuszak, G. Y. Yin, and S. E. Harris, Phys. Rev. Lett. **84**, 5308 (2000).

[5] H. Wang, D. Goorskey, and M. Xiao, Phys. Rev. Lett. **87**, 073601 (2001).

[6] A. V. Turukhin *et al.*, Phys. Rev. Lett. **88**, 023602 (2002).

[7] A. B. Matsko, O. Kocharovskaya, Y. Rostovtsev, G. R. Welch, A. S. Zibrov, and M. O. Scully, Adv. At., Mol., Opt. Phys. **46**, 191 (2001).

[8] C. Liu, Z. Dutton, C. H. Behroozi, and L. V. Hau, Nature (London) **409**, 490 (2001).

[9] D. F. Phillips, A. Fleischhauer, A. Mair, R. L. Walsworth, and M. D. Lukin, Phys. Rev. Lett. **86**, 783 (2001).

[10] A. S. Zibrov, A. B. Matsko, O. Kocharovskaya, Y. V. Rostovtsev, G. R. Welch, and M. O. Scully, Phys. Rev. Lett. **88**, 103601 (2002).

[11] S. E. Harris and Y. Yamamoto, Phys. Rev. Lett. **81**, 3611 (1998).

[12] S. E. Harris and L. V. Hau, Phys. Rev. Lett. **82**, 4611 (1999).

[13] M. D. Lukin and A. Imamoglu, Phys. Rev. Lett. **84**, 1419 (2000).

[14] M. Jain, H. Xia, G. Y. Yin, A. J. Merriam, and S. E. Harris, Phys. Rev. Lett. **77**, 4326 (1996).

[15] K. Hakuta, L. Marmet, and B. P. Stoicheff, Phys. Rev. A **45**, 5152 (1992).

[16] S. E. Harris and A. V. Sokolov, Phys. Rev. Lett. **81**, 2894 (1998).

[17] M. O. Scully, G. W. Kattawar, P. R. Lucht, T. Opatrny, H. Pilloff, A. Rebane, A. V. Sokolov, and M. S. Zubairy, Proc. Natl. Acad. Sci. U.S.A. **9**, 10994 (2002).

[18] N. V. Vitanov, M. Fleischhauer, B. W. Shore, and K. Bergmann, Adv. At., Mol., Opt. Phys. **46**, 55 (2001).

[19] A. T. Nguyen, G. D. Chern, D. Budker, and M. Zolotorev, Phys. Rev. A **63**, 013406 (2000).

[20] R. Netz, A. Nazarkin, and R. Sauerbrey, Phys. Rev. Lett. **90**, 063001 (2003).

[21] C. Y. Ye, V. A. Sautenkov, Y. V. Rostovtsev, and M. O. Scully, Opt. Lett. **28**, 2213 (2003).

[22] A. E. Johnson, E. S. Maniloff, and T. W. Mossberg, Opt. Lett. **24**, 1526 (1999).

[23] V. A. Sautenkov, M. M. Kash, V. L. Velichansky, and G. R. Welch, Laser Phys. **9**, 1 (1999).

[24] E. Arimondo, in *Progress in Optics*, edited by E. Wolf (Elsevier Science, Amsterdam, 1996), p. 257.

[25] R. Buffa, M. P. Anscombe, and J. P. Marangos, Phys. Rev. A **67**, 033801 (2003).

[26] L. Deng, M. G. Payne, and W. R. Garrett, Phys. Rev. A **63**, 043811 (2001).

[27] G. Beadie, J. Reintjes, M. Bashkansky, T. Opatrny, and M. O. Scully, J. Mod. Opt. **50**, 2361 (2003).

[28] B. Bosacchi, M. Mehendale, W. S. Warren, H. Rabitz, and M. O. Scully, Proc. SPIE **5200**, 31 (2003).

[29] M. Mehendale, B. Bosacchi, W. S. Warren, and M. O. Scully, Proc. SPIE **5200**, 46 (2003).